Gynecologic Oncology 173 (2023) 31–40

Contents lists available at ScienceDirect

Gynecologic Oncology

journal homepage: www.elsevier.com/locate/ygyno

Downregulating vaccinia-related kinase 1 by luteolin suppresses ovarian cancer cell proliferation by activating the p53 signaling pathway

Xuboya Chang [a], Satoshi Tamauchi [a,*], Kosuke Yoshida [a,b], Masato Yoshihara [a], Akira Yokoi [a,b], Yusuke Shimizu [a], Yoshiki Ikeda [a], Nobuhisa Yoshikawa [a], Tohru Kiyono [d], Yusuke Yamamoto [c], Hiroaki Kajiyama [a]

[a] Department of Obstetrics and Gynecology, Nagoya University Graduate School of Medicine, Nagoya 466-8550, Japan
[b] Institute for Advanced Research, Nagoya University, Nagoya 464-8601, Japan
[c] Laboratory of Integrative Oncology, National Cancer Center Research Institute, Tokyo 104-0045, Japan
[d] Project for Prevention of HPV-related Cancer, Exploratory Oncology Research and Clinical Trial Center, Chiba 277-8577, Japan

HIGHLIGHTS

- Blocking the VRK1 pathway via siVRK1 decreasedecreases the proliferation of HGSOC cells.
- Using luteolin alone and in combination with cisplatin inhibits tumor growth in vitro.
- The IP of luteolin plus cisplatin shows an additive effect on ovarian cancer inhibition.
- Oral administration of luteolin can decrease the proliferation of ovarian cancer.

ARTICLE INFO

Article history:
Received 22 December 2022
Received in revised form 10 March 2023
Accepted 3 April 2023
Available online xxxx

Keywords:
Ovarian cancer
Luteolin
Vaccinia-related kinase
Patient-derived xenograft
Flavonoid

ABSTRACT

Objectives. Ovarian cancer constitutes one of the most common causes of cancer-related deaths, and preventing chemotherapy resistance and recurrence in patients with ovarian cancer remains a challenge. Herein, we aimed to identify the effect of luteolin, a novel therapeutic agent targeting vaccinia-related kinase 1 (VRK1), on high-grade serous ovarian cancer (HGSOC).

Methods. Phosphokinase array, RNA sequencing, and cell cycle and apoptosis assays were conducted to determine the underlying mechanism of the effect of luteolin on HGSOC cells. The anticancer effects of oral and intraperitoneal luteolin administration were assessed in patient-derived xenograft models via several methods, including the assessment of tumor size and immunohistochemistry of phospho-p53, phosphor-HistoneH3 and cleaved caspase 3.

Results. Luteolin reduced HGSOC cell proliferation and increased apoptosis and cell cycle arrest at G2/M. Compared with controls, several genes were dysregulated in luteolin-treated cells, and luteolin activated the p53 signaling pathway. The human phosphokinase array revealed distinct p53 upregulation in luteolin-treated cells, as confirmed by p53 phosphorylation at ser15 and ser46 using western blot analysis. In patient-derived xenograft models, oral or intraperitoneal luteolin administration substantially suppressed tumor growth. Moreover, combination treatment involving luteolin and cisplatin inhibited tumor cell proliferation, especially in cisplatin-resistant HGSOC cell lines.

Conclusions. Luteolin demonstrated considerable anticancer effect on HGSOC cells, reduced VRK1 expression, and activated the p53 signaling pathway, thereby inducing apoptosis and cell cycle arrest in G2/M and inhibiting cell proliferation. Furthermore, luteolin exhibited a synergistic effect with cisplatin both in vivo and in vitro. Thus, luteolin can be considered a promising cotreatment option for HGSOC.

1. Introduction

Ovarian cancer is a major cause of mortality among gynecological malignancies [1]. More than half of the patients with ovarian cancer are diagnosed at an advanced stage owing to the asymptomatic nature

* Corresponding author at: Department of Obstetrics and Gynecology, Nagoya University Graduate School of Medicine, 65 Tsuruma-cho, Showa-ku, Nagoya 466-8550, Japan.
E-mail address: tama-sato@med.nagoya-u.ac.jp (S. Tamauchi).

https://doi.org/10.1016/j.ygyno.2023.04.003
0090-8258/

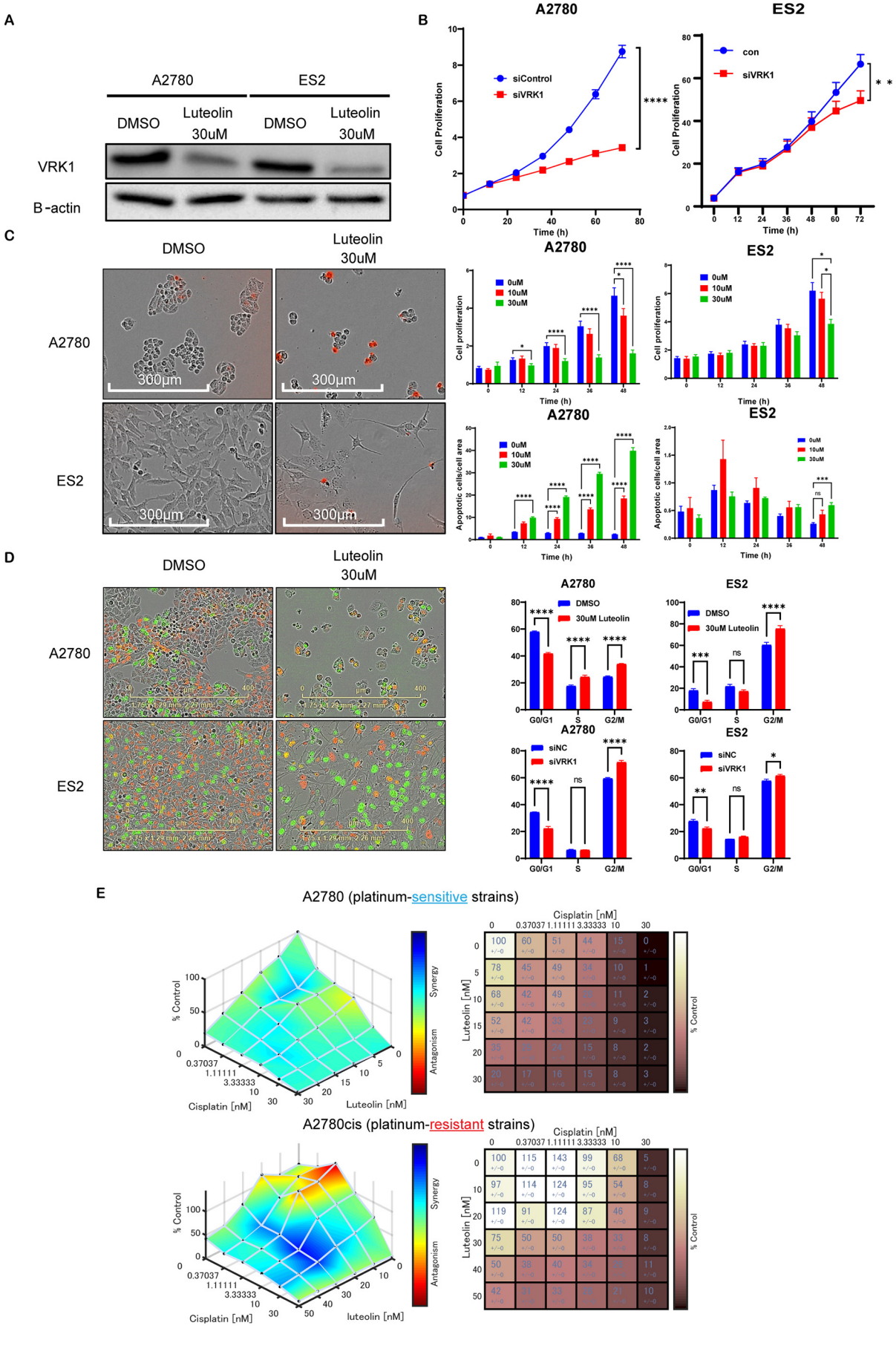
A
A2780
ES2
DMSO
Luteolin 30uM
DMSO
Luteolin 30uM
VRK1
B-actin
B
A2780
ES2
siControl
siVRK1
Cell Proliferation
Time (h)
****
con
siVRK1
* *
C
DMSO
Luteolin 30uM
A2780
ES2
300μm
0uM
10uM
30uM
Cell proliferation
Time (h)
Apoptotic cells/cell area
D
DMSO
Luteolin 30uM
A2780
ES2
DMSO
30uM Luteolin
G0/G1
S
G2/M
siNC
siVRK1
E
A2780 (platinum-sensitive strains)
Cisplatin [nM]
Luteolin [nM]
% Control
Synergy
Antagonism
A2780cis (platinum-resistant strains)

of the disease and lack of effective early detection methods [2]. Despite the high initial response rate (~80%) to carboplatin and paclitaxel chemotherapy, ovarian cancer eventually recurs and is accompanied by acquired chemotherapy resistance [3]. Recently developed molecular targeting agents, such as bevacizumab and poly(ADP-ribose) polymerase inhibitors, have proven effective at extending the recurrence time. However, it remains challenging to completely prevent recurrence, and hence, novel treatment options are warranted.

An epidemiological study in the UK reported that consuming vegetables and fruits was associated with reduced mortality rates, especially for cancer (hazard ratio 0.75 [95% confidence interval 0.59–0.96]) [4]. However, owing to the large scale of this study, it remains unclear which components of fruits and vegetables were the most effective against cancer. Nevertheless, among those components, luteolin, a flavonoid, has been studied for its health benefits, such as preventing type 2 diabetes mellitus [5] and various cancers, including gastric cancer [6–8], colorectal carcinoma [9] and bladder cancer [10]. However, it has not yet been used to treat human patients with cancer.

Inhibiting vaccinia-related kinase (VRK1) is an underlying mechanism of the antitumor effects of luteolin [11,12]. VRK1 is a serine/threonine kinase[13,14). identified as a novel therapeutic target in a comprehensive knockdown screening involving ovarian cancer cell lines [15] Although VRK1 is a potential therapeutic target for other cancer types [13], specific inhibitors are yet to be developed [16]. An analysis of the Gene Expression Profiling Interactive Analysis database (http://gepia.cancer-pku.cn/) revealed that cancer cells exhibit higher VRK1 expression than normal cells.

p53 is a critical tumor suppressor protein and target of VRK1 that controls cell cycle, DNA repair, and uncontrolled cell division during tumor growth [17]. Following mild DNA damage, p53 triggers cell cycle arrest by phosphorylating the ser15 of p53 and inducing p21 expression. However, in the event of severe DNA damage, p53 triggers apoptosis by phosphorylating both ser15 and ser46 of p53 [18].

Patient-derived xenografts (PDX) are cancer models wherein tissue or cells are obtained from patient tumors and implanted onto an immunodeficient or humanized mouse. This can be a promising tool for preclinical drug screening [19–21]. Herein, we used A2780 and ES2, which are high-grade serous ovarian cancer (HGSOC) cell lines, and the TIL15 PDX model to test the effect of luteolin in vitro or in vivo. We demonstrated the efficacy of luteolin in HGSOC, its action mechanism after activating VRK1 inhibition, and its efficacy in PDX models. Our results demonstrated that oral luteolin therapy is a promising treatment option for HGSOC.

2. Materials and methods

2.1. Cell culture and reagents

The human ovarian cancer cell lines ES2 and A2780 were purchased from the American Type Culture Collection and maintained in Dulbecco's modified eagle medium and RPMI 1640, respectively, supplemented with 10% fetal bovine serum (FBS). Cisplatin-resistant (A2780cis) human ovarian cancer cells, purchased from the European Collection of Authenticated Cell Cultures, were maintained in RPMI 1640 supplemented with 10% FBS. Normal ovarian surface cell lines, HOSE1C and HOSE2C, were established using mutant CDK4, cyclin D1, and telomerase reverse transcriptase via lentvirus-mediated gene transfer [22]. The TP53 status of all cells is shown in Supplementary Fig. 1. All cells were cultured at 37 °C in a humidified atmosphere containing 95% air and 5% CO_2. Purified luteolin was purchased from Abcam (ab120662) and dissolved in dimethyl sulfoxide (DMSO) before use.

2.2. Transfection

To knockdown small interfering RNA (siRNA), cells were transfected with human VRK1 or negative control siRNA (Thermo Fisher Scientific) using Lipofectamine RNAiMAX (Thermo Fisher Scientific). After 24 h of transfection, the cells were cultured in RPMI 1640 for 72 h. Human VRK1 shRNA lentiviral plasmids and control shRNA were purchased from VectorBuilder (Kanagawa, Japan) and transfected into Lenti-X 293 T cells (Clontech). Then, A2780 cells were infected with pseudovirus particles to which polybrene (8 μg/mL) was added. Subsequently, the cells were treated with puromycin (4 μg/mL) for 72 h to select the stably infected cells.

2.3. Cell proliferation assay

ES2 and A2780 cells were seeded into 96-well plates at a density of 2000 cells/well. After 24 h, the cells were treated with luteolin. Then, the plate was moved into IncuCyte ZOOM (Essen BioScience, Ann Arbor, MI, USA) for live-cell imaging. The images of each well were recorded every hour for a total of 72 h. Finally, IncuCyte ZOOM 2018 software was used to determine the confluence of each well. Cell proliferation was measured using 3-(4,5-dimethylthiazol-2-yl)-5-(3-carboxymethoxyphenyl)-2-(4-sulfophenyl)-2H-tetrazolium, inner salt (MTS) assay. After 72 h of incubation, 15 μL 5 mg/mL CellTiter 96 Aqueous One Solution (Promega, Madison, WI, USA) was added to each well and incubated for 1 h. The optical density of each well was measured at a wavelength of 490 nm using a spectrophotometer. All experiments were performed in triplicate.

2.4. Apoptosis assay and cell cycle analysis

Cells (4.5×10^5) were seeded into 6-well plates. After 24 h, the respective drugs were administered. After 72 h, the cells were collected. Incucyte Annexin V RED reagent was used for apoptosis assays according to the manufacturer's instructions. All experiments were performed in triplicate. For the cell cycle experiment, Incucyte cell cycle G/R lentivirus was employed to transfect the cells. Incucyte SX5 (Sartorius, Johnson Avenue, Bohemia, USA) was used to record the images of each well every 30 min for a total of 72 h. Lastly, confluence and fluorescence of the cells were determined using Incucyte 2018 software.

2.5. Western blot analysis

Cells (4.5×10^5) were seeded into 6-well plates. After 24 h, the respective drugs were administered. After 72 h, the cells were washed twice with phosphate-buffered saline (PBS) and lysed using cell lysis buffer for 30 min on ice. The samples were centrifuged at 15,000 rpm for 10 min and the supernatant was collected. Following sodium dodecyl sulfate–polyacrylamide gel electrophoresis, the proteins were transferred on the membrane and blocked for 1 h with 5% milk in PBS containing 0.1% Tween-20 at room temperature and then incubated with primary antibodies against VRK1 (1:1000; #3307; Cell Signaling Technology [CST]), phosphor-Histone H3 (1:1000; #9701; CST), p53 (1:1000; #B0222; Santa Cruz), phophos-p53 ser15 (1:1000; #9284;

Fig. 1. Luteolin exhibits a suppressive effect on human ovarian cancer cells.
A. Western blot analysis of VRK1 in A2780 and ES2 cells treated with luteolin.
B. Cell viability of A2780 and ES2 cells after treatment with siVRK1 for 72 h.
C. Apoptosis of A2780 and ES2 cells detected using Annexin V via Incucyte.
D. Cell cycle assay of cells treated with cell cycle lentivirus reagents.
E. Cells were treated with the indicated drugs for 72 h, and the percentage of viable cells was determined using Combenefit software. All experiments were performed in triplicate.

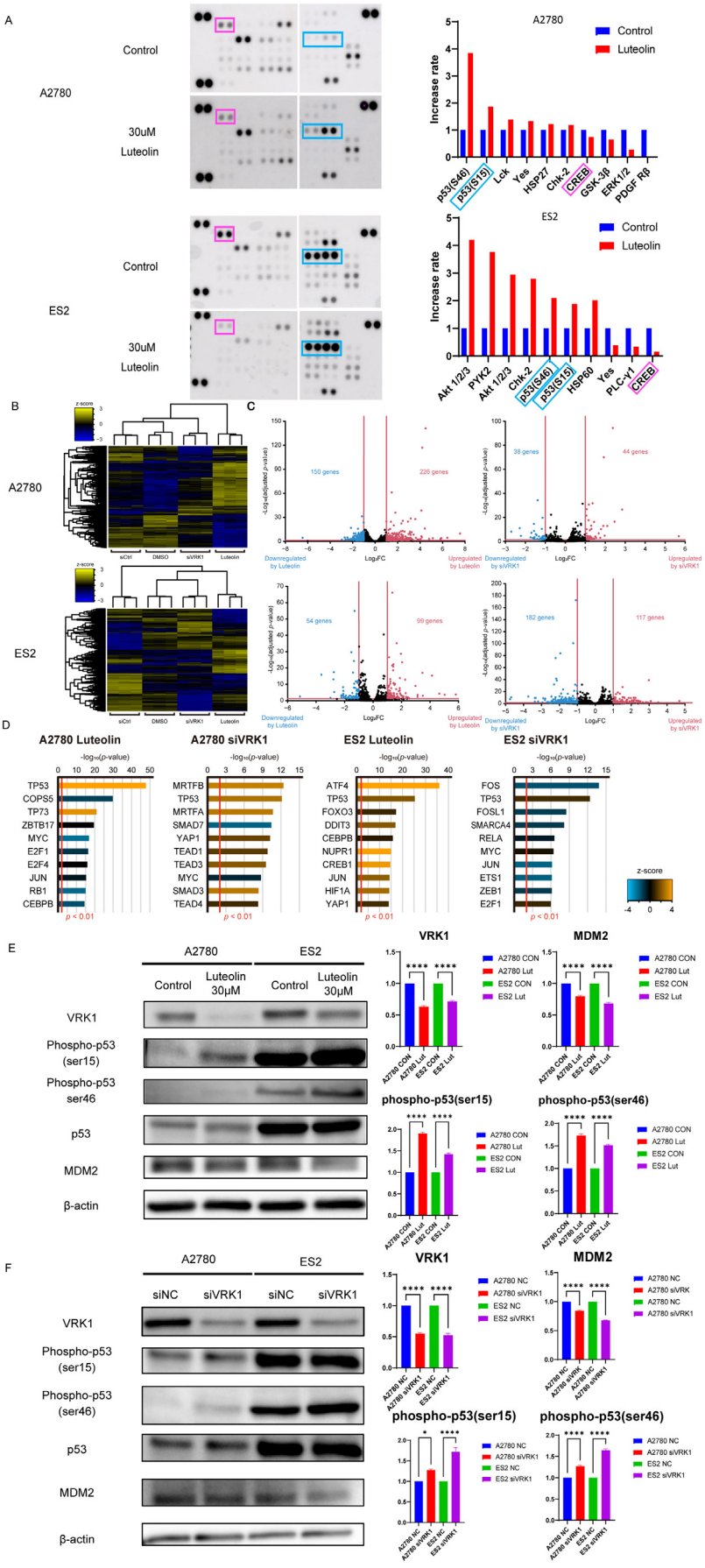
A
A2780
Control
30uM Luteolin
ES2
Control
30uM Luteolin
A2780
Control
Luteolin
Increase rate
p53(S46)
p53(S15)
Lck
Yes
HSP27
Chk-2
CREB
GSK-3β
ERK1/2
PDGF Rβ
ES2
Control
Luteolin
Increase rate
Akt 1/2/3
PYK2
Akt 1/2/3
Chk-2
p53(S46)
p53(S15)
HSP60
Yes
PLC-γ1
CREB
B
A2780
ES2
z-score
siCtrl
DMSO
siVRK1
Luteolin
C
150 genes
226 genes
38 genes
44 genes
54 genes
99 genes
182 genes
117 genes
-Log10(adjusted p-value)
Log2FC
Downregulated by Luteolin
Upregulated by Luteolin
Downregulated by siVRK1
Upregulated by siVRK1
D
A2780 Luteolin
A2780 siVRK1
ES2 Luteolin
ES2 siVRK1
-log10(p-value)
TP53
COPS5
TP73
ZBTB17
MYC
E2F1
E2F4
JUN
RB1
CEBPB
MRTFB
TP53
MRTFA
SMAD7
YAP1
TEAD1
TEAD3
MYC
SMAD3
TEAD4
ATF4
TP53
FOXO3
DDIT3
CEBPB
NUPR1
CREB1
JUN
HIF1A
YAP1
FOS
TP53
FOSL1
SMARCA4
RELA
MYC
JUN
ETS1
ZEB1
E2F1
p < 0.01
z-score
E
A2780
ES2
Control
Luteolin 30μM
Control
Luteolin 30μM
VRK1
Phospho-p53 (ser15)
Phospho-p53 ser46
p53
MDM2
β-actin
VRK1
MDM2
phospho-p53(ser15)
phospho-p53(ser46)
A2780 CON
A2780 Lut
ES2 CON
ES2 Lut
F
A2780
ES2
siNC
siVRK1
siNC
siVRK1
VRK1
Phospho-p53 (ser15)
Phospho-p53 (ser46)
p53
MDM2
β-actin
VRK1
MDM2
phospho-p53(ser15)
phospho-p53(ser46)
A2780 NC
A2780 siVRK1
ES2 NC
ES2 siVRK1

CST), phophos-p53 ser46 (1:1000; #2521; CST), MDM2 (1:1000; #H2521; Santa Cruz), and p21 (1:1000; #L2921; Santa Cruz) overnight at 4 °C. The membranes were incubated with the appropriate secondary antibodies against anti-mouse IgG (1:1000; #7076S, CST), anti-rabbit IgG (1:1000, #7074S, CST), and horseradish peroxidase. The bands were visualized via chemiluminescence using ImageQuant LAS400 mini Machine and ImageQuant LAS400 Analysis Software. ImageJ software was used to quantitate the results of the western blots with β-actin as an internal control. All experiments were performed in triplicate.

2.6. Human phosphokinase array

The relative levels of protein phosphorylation were determined using Proteome Profiler Human Phosphokinase Array kit (Cat#: ARY003B; R&D Systems, Minneapolis, USA). Cell lysate protein (300 μg) was incubated in an 8-well multidish precoated with specific antibodies at 4 °C overnight. After washing, each well was incubated with biotin-labeled antibodies for 2 h at room temperature and then incubated with horseradish peroxidase–streptavidin for 30 min on a rocking platform at room temperature. Chemiluminescence and spot pixel density were measured using Amersham 18 Imager 600 (GE Healthcare).

2.7. RNA sequencing analysis

The total RNA was extracted from A2780 and ES2 cells treated with DMSO, luteolin, siNegative control, and siVRK1 using miRNeasy Mini Kit (Qiagen). RNA-seq analysis was performed by the Novogene company. The expression levels of each gene were quantified from the sequencing data using Kallisto. Employing the tximport package (ver. 1.18.0) for R software (ver. 4.0.3) and RStudio (Rstudio) to further process the data, transcripts per million counts was used for further analysis. Low-read coverage (maximum read count: <10 reads) genes were excluded, and differentially expressed genes (DEGs, $|\log2FC| > 1$) between the A2780 and ES2 were used for heatmap analysis. After the data was converted to base 10 logarithms and z-scores, the heatmap.2 function of gplots package (ver. 3.1.0) for R was used. For volcano plots, the adjusted *p*-values for each gene were calculated using Wald test in DESeq2 (ver. 1.34.0). Subsequently, Ingenuity Pathway Analysis (Qiagen) was performed using the significant DEGs identified from the volcano plot.

2.8. Ex vivo experiment

Ovarian cancer tissues from PDX model samples ($n = 3$) were collected prospectively, following the protocol approved by the Ethics Committee of Nagoya University (Approval no. 22015–0237). The collected samples were stored in STEM-CELLBANKER GMP grade (Catalog CB047, TAKARA) and frozen at −80 °C. Sample processing was performed as reported previously [23]. After thawing, the tissue was cut into 1 mm^3 pieces using a scalpel, and 3–4 pieces/sponge for each treatment were explanted onto AteloCell (Catalog CSH-96, KOKEN) in 96-well plates immersed in 70–100 μL of RPMI-1640 media supplemented with 10% FBS and antibiotics in addition to DMSO luteolin (30 μM, dissolved in DMSO, Shinsei Chemical Company Ltd.) in a humidified atmosphere at 37 °C containing 5% CO_2. Tissues were harvested after 48–72 h and fixed with 4% buffered formalin.

2.9. Animals

Four-week-old female NSG (NOD.Cg-Prkdc^{scid}Il2rg^{tm1Wjl}/SzJ) and BALB/c nude mice were procured from Oriental BioService, Inc. and maintained in a temperature-controlled, pathogen-free environment with a 12-h light/dark cycle and fed autoclaved water and irradiated food. All animal experiments were approved by the Animal Care and Use Committee of the Nagoya University Graduate School of Medicine (Nagoya, Japan).

2.10. PDX model

In previous experiments, our department has established numerous PDX models [24]. TIL4 is a PDX model of ovarian endometrioid carcinoma. TIL5 and TIL15 are PDX models of high-grade ovarian serous carcinoma. The expression of VRK1 of three PDX models was shown in Supplementary Fig. 4. TIL15 was used for the mouse experiment due to its highly expresses VRK1. And the whole exome sequencing for TIL15 was shown in Supplementary Fig. 5.

Patient-derived tumors were grown in vivo in NSG mice, and then these were split and transplanted into nude mice for animal experiments. To create PDX nude mice, tumors excised from TIL15-NSG mice were immediately cut into small sections, immersed in PBS, and then implanted subcutaneously in the flank regions of anesthetized nude mice. When the tumor size reached 100 cm^3, the mice were divided into groups with the same average tumor size. Tumor size was measured weekly. Tumor volume was calculated using the following formula: ½ × length × width × height. The establishment of PDX models was approved by the Committee of the Nagoya University Graduate School of Medicine (Nagoya, Japan).

2.11. Immunohistochemical staining

Paraffin-embedded blocks were sliced into 4-μm sections and mounted onto slides. Following deparaffinization and antigen retrieval, the tissues were incubated with antibodies against Histone H3 (1:100; #9701; CST), phospho-p53 ser15 (1:100; #9284; CST), or cleaved caspase 3 (1:400, #9661, CST) overnight at 4 °C. After washing with PBS and tween, the tissues were incubated with the corresponding secondary antibodies for 10 min at 37 °C. Finally, the sections were stained using a DAB staining solution and counterstained with hematoxylin.

3. Results

3.1. Effects of luteolin-induced VRK1 downregulation on A2780 and ES2 cell viability

Western blot analysis revealed that luteolin significantly decreased VRK1 expression (Fig. 1A). Cell proliferation was decreased by siVRK1

Fig. 2. Luteolin increases p53 phosphorylation.
A. Human phosphokinase array using A2780 cells after silencing VRK1 and treatment with luteolin. The bar graph shows the top 15 upregulated proteins.
B. Hierarchical clustering and heatmap showing the difference between the siCtrl-, siVRK1-, DMSO-, and luteolin-treated groups. The 869 genes were defined as an absolute log2-fold change >1.
C. Volcano plot showing significant DEGs between the siCtrl-, siVRK1-, DMSO-, and luteolin-treated groups in A2780 and ES2 cells. The adjusted *P*-values for each gene were calculated using Wald test in DESeq2.
D. Top 10 significantly altered pathways.
E. Western blot analysis of the p53 signaling pathway and VRK1 in A2780 and ES2 cells treated with luteolin. $^{*}P < 0.05$, $^{**}P < 0.01$, $^{***}P < 0.001$, $^{****}P < 0.0001$, unpaired, one-way analysis of variance (ANOVA) analysis. Error bars in all data indicate mean ± SEM.
F. Western blot analysis of the p53 signaling pathway and VRK1 in A2780 and ES2 cells treated with siVRK1. $^{*}P < 0.05$, $^{**}P < 0.01$, $^{***}P < 0.001$, $^{****}P < 0.0001$, unpaired, one-way ANOVA analysis. Error bars in all data indicate mean ± SEM.

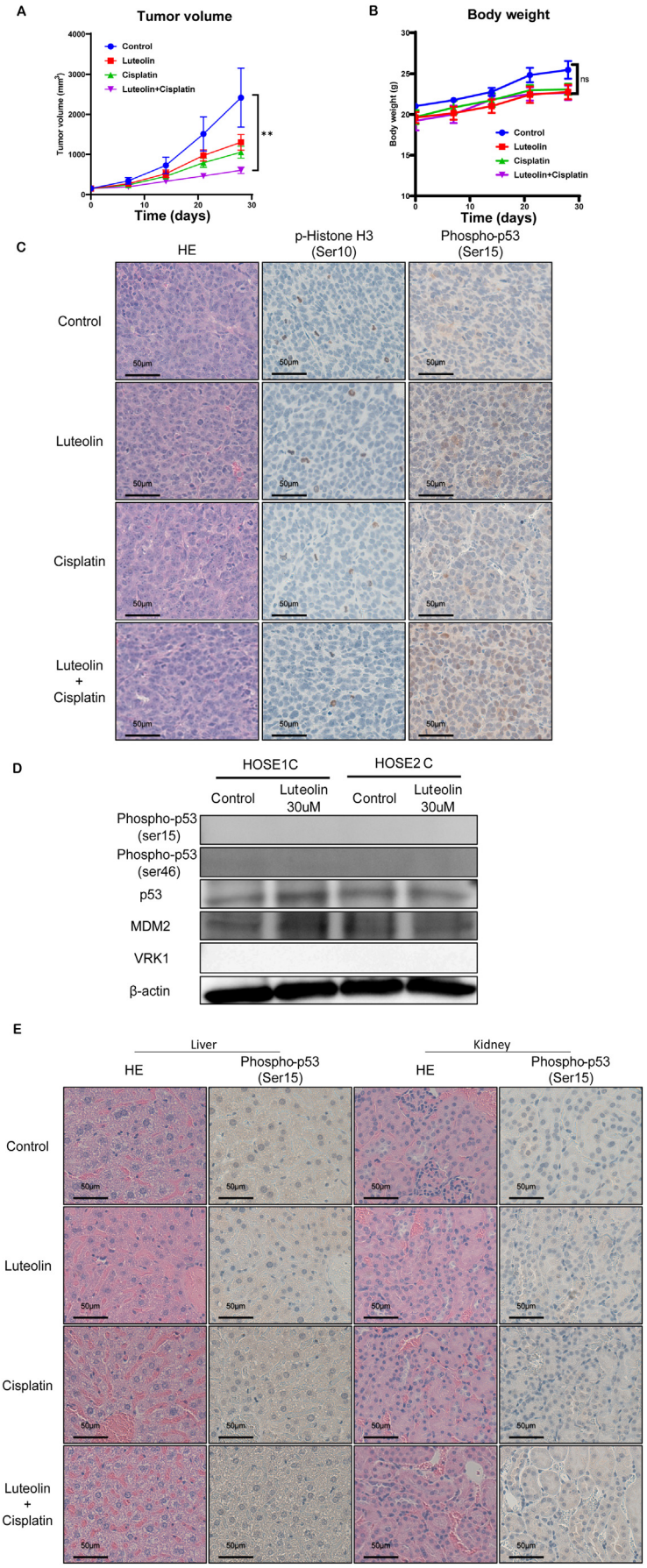
A
Tumor volume
Control
Luteolin
Cisplatin
Luteolin+Cisplatin
Tumor volume (mm³)
Time (days)
**
B
Body weight
Body weight (g)
Time (days)
ns
C
HE
p-Histone H3 (Ser10)
Phospho-p53 (Ser15)
Control
Luteolin
Cisplatin
Luteolin + Cisplatin
50μm
D
HOSE1C
HOSE2 C
Control
Luteolin 30uM
Phospho-p53 (ser15)
Phospho-p53 (ser46)
p53
MDM2
VRK1
β-actin
E
Liver
Kidney
HE
Phospho-p53 (Ser15)
Control
Luteolin
Cisplatin
Luteolin + Cisplatin

(Fig. 1B). We further determined the inhibitory effects of luteolin on A2780 and ES2 ovarian cancer cell viability. Luteolin dose- and time-dependent decreased HGSOC cell viability (Fig. 1C). We also tested the effect of luteolin on other cell lines, endometrial cancer cell lines, and cervical cell lines (Supplementary Fig. 2). To determine the mechanism through which luteolin inhibits cell viability, apoptosis and cell cycle assays were conducted (Fig. 1C, D). Fig. 1C shows that luteolin increased apoptosis in A2780 and ES2 cells. The cell cycle assays revealed that both luteolin and siVRK1 induced G2/M arrest in A2780 and ES2 cells.

Several studies have suggested that VRK1 is vital for promoting chemotherapy resistance [12,13,25] Therefore, we investigated whether luteolin, which inhibits VRK1 expression, could circumvent chemotherapeutic drug resistance. We assessed the effects of luteolin and cisplatin combination therapy. The proliferation of the cells treated with various doses of luteolin (0, 5, 10, 15, 20, or 30 μM) and cisplatin (0, 0.37, 1.11, 3.33, or 10 μM) for 72 h was measured using MTS assay (Fig. 1E). Luteolin treatment only inhibited cell proliferation in a dose-dependent manner in both A2780 and A2780cis cells. The cells treated for 72 h with different combinations of luteolin and cisplatin exhibited a significant decrease in proliferation compared with the cells treated with luteolin or cisplatin alone.

3.2. Luteolin activates the p53 signaling pathway

To further investigate the functional role of luteolin in HGSOC treatment, Proteome Profiler Human Phosphokinase Array and RNA-seq were performed. Luteolin activated several phosphokinase proteins, including p53(s15) and p53(s46), and inhibited the expression of several phosphokinase proteins, such as CREB and ERK1/2. The heatmap showed 869 DEGs (absolute log2 fold change >1) in A2780 cells treated with DMSO, luteolin, siCtrl, and siVRK1, and 903 DEGs (absolute log2 fold change >1) in ES2 cells treated with DMSO, luteolin, siCtrl, and siVRK1 (Fig. 2B). Subsequently, multivariate analysis was performed to compare the expression of multiple genes shown in the heat map of A2780 and ES2 cells (Fig. 2C). In A2780 cells treated with DMSO or luteolin, 226 and 150 genes were significantly upregulated and downregulated, respectively ($|\log2FC| > 1$, adjusted P value of <0.05). In A2780 cells treated with siCtrl or siVRK1, 44 and 38 genes were significantly upregulated and downregulated, respectively ($|\log2FC| > 1$, adjusted P value of <0.05). In ES2 cells treated with DMSO or luteolin, 99 and 54 genes were significantly upregulated and downregulated, respectively ($|\log2FC| > 1$, adjusted P value of <0.05). In ES2 cells treated with siCtrl or siVRK1, 117 and 182 genes were significantly upregulated and downregulated, respectively ($|\log2FC| > 1$, adjusted P value of <0.05). Via Ingenuity Pathway Analysis of the luteolin group, we found that p53 activity was activated by luteolin in both A2780 and ES2 cells compared with the control A2780 and ES2 cells (Fig. 2D). This corresponded with the results of the phosphorylation assay. Ingenuity Pathway Analysis between the cells treated with siVRK1 and negative control (siCtrl) revealed that siVRK1 promoted p53 activity in A2780 cells; however, it lightly promoted p53 activity in ES2 cells.

Western blot analysis (Fig. 2E, F) confirmed these findings and further revealed that both luteolin and siVRK1 increased p53 phosphorylation at ser15 and ser 46 and decreased MDM2 expression compared to controls. These findings indicate that luteolin decreases cell proliferation by targeting VRK1.

The result of the immunohistochemistry of TIL4, TIL5, and TIL15 ex vivo experiments are shown in Supplementary Fig. 3. Luteolin decreased the expression of phospho-Histone H3 and increased the expression of phosphor-p53(ser15) and cleaved caspase 3. These results indicate that luteolin decreases cell proliferation in ex vivo experiments.

3.3. Luteolin suppresses tumor growth in vivo

To better understand the effects of luteolin on tumor growth in vivo, a PDX model was established. After tumors were formed, nude mice were divided into four groups (control group, 10 mg/kg luteolin, 0.5 mg/kg cisplatin, and 10 mg/kg luteolin plus 0.5 mg/kg cisplatin; $n = 5$/group) and administered their respective injections once per week intraperitoneally for 4 weeks. Tumor size was measured once a week. At the end of the experiment, all mice were euthanized and tumor tissue was extracted (Fig. 3A–C). The growth of the tumor size in the luteolin-treated group was slower than that in the control group (Fig. 3 A). The tumor volume in the luteolin-treated group was lesser than that in the control group (Fig. 3B). The growth of the tumor size in the luteolin plus cisplatin-treated group was slower than that in the cisplatin only-treated group. Tumor volume and weight in the luteolin plus cisplatin-treated group were lesser than that in the cisplatin only-treated group. Furthermore, immunohistochemistry was employed to analyze protein expression in the tumor tissue samples (Fig. 3D). Histone H3 phosphorylation was decreased while p53 phosphorylation was increased in tumors in the luteolin-treated group than in the control group. Furthermore, histone H3 phosphorylation decreased and p53 phosphorylation increased in tumors in the luteolin plus cisplatin-treated group than in the cisplatin only-treated group. p53 phosphorylation remained unchanged in the liver and kidneys (Fig. 3F). Western blot analysis using HOSE1C and HOSE2C cells with or without luteolin treatment also shows that the phosphorylation of p53 at ser15 and ser46 remained unchanged (Fig. 3E). Furthermore, the body weight of mice was not significantly different between the control and luteolin groups (Fig. 3C). These findings suggest that luteolin is not toxic to normal tissues.

3.4. Oral luteolin therapy suppresses tumor growth in vivo

Luteolin is a flavonoid present in numerous vegetables, such as celery, broccoli, and peppers, and thus we examined whether oral luteolin suppressed tumor growth using a PDX model. After the tumors were formed, nude mice were divided into two groups ($n = 6$/group) and fed a normal diet or a diet including luteolin (50 ppm) for 4 weeks. Tumor growth in mice administered with oral luteolin therapy was slower than in controls (Fig. 4A–C). Furthermore, immunohistochemistry revealed that histone H3 phosphorylation decreased and p53 phosphorylation increased in the tumors of the mice administered with luteolin therapy (Fig. 4D).

4. Discussion

Previous studies have reported that VRK1 is crucial for regulating various cellular activities. In cancer, VRK1 expression has been associated with disease progression and prognosis. Furthermore, it has been linked with chemotherapy resistance [12]. Luteolin, a flavonoid present in vegetables, exhibits anticancer properties [26] and reportedly decreases VRK1 expression [11].

Cell proliferation constitute a sign of tumor progression [27]. On examining the effects of luteolin on HGSOC cell proliferation, we

Fig. 3. Luteolin suppresses tumor growth in vivo.
A. Tumor volume of mice treated with PBS, luteolin, cisplatin, and luteolin plus cisplatin combination therapy ($n = 5$/group).
B. Body weight of the mice.
C. Expression of phosphorylated histone H3 (ser10) and phosphorylated p53 (ser53) in tumors from a PDX model via immunohistochemistry.
D. Western blot analysis of the p53 signaling pathway and VRK1 in HOSE1C and HOSE2C cells treated with luteolin.
E. Expression of phosphorylated histone H3 (ser10) and phosphorylated p53 (ser53) in the liver and kidneys from PDX model mice via immunohistochemistry. Scale bar: 50 um.

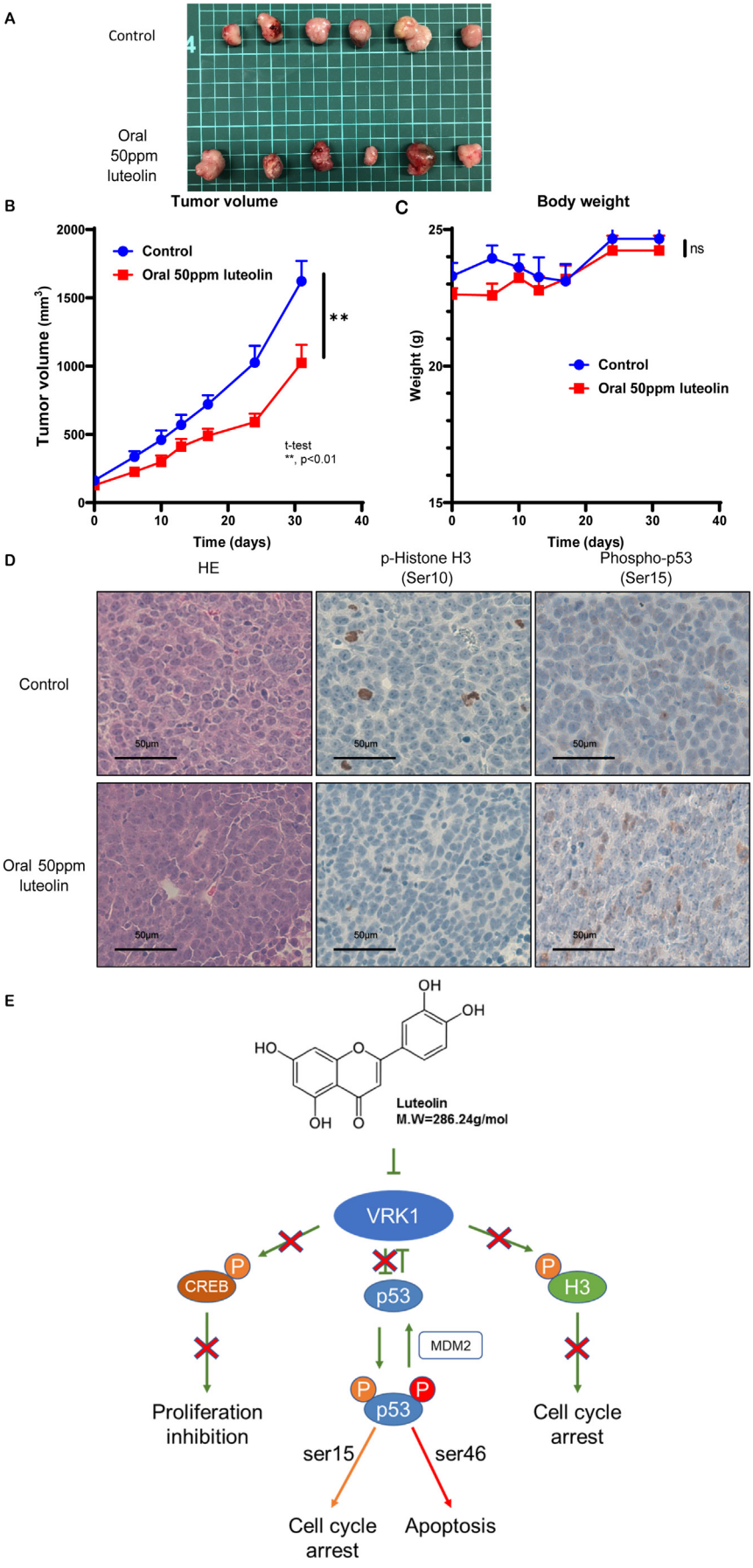
A
Control
Oral 50ppm luteolin
B
Tumor volume
Control
Oral 50ppm luteolin
Tumor volume (mm3)
Time (days)
**
t-test
**, p<0.01
C
Body weight
Weight (g)
Time (days)
ns
Control
Oral 50ppm luteolin
D
HE
p-Histone H3 (Ser10)
Phospho-p53 (Ser15)
Control
Oral 50ppm luteolin
50μm
E
Luteolin
M.W=286.24g/mol
VRK1
CREB
H3
p53
MDM2
Proliferation inhibition
Cell cycle arrest
ser15
ser46
Cell cycle arrest
Apoptosis

observed that luteolin significantly decreases HGSOC cell proliferation in a time- and dose-dependent manner. The cell cycle and apoptosis assays revealed that luteolin induces G2/M cell cycle arrest and promotes apoptosis. Several studies have reported that chromatin condensation requires VRK1 during G2/M and apoptosis [14]. These results indicate that luteolin inhibits cell proliferation by inhibiting VRK1 expression (Fig. 4E).

The most common chemotherapeutic treatment for ovarian cancer relies on platinum-based drugs [28]. Chemotherapy resistance constitutes a major clinical issue in patients with ovarian cancer. VRK1 is crucial for promoting cisplatin resistance [29]. Therefore, we aimed to determine whether luteolin could reverse drug resistance by inhibiting VRK1. Our results showed that luteolin dose-dependently augmented the effect of cisplatin, which inhibits A2780 and cisplatin-resistant A2780cis cell proliferation. This indicates the synergistic effect of luteolin when combined with cisplatin in vitro. The combination of luteolin and cisplatin will be a new strategy for HGSOC.

To determine the action mechanism of the effects of luteolin, we used Proteome Profiler Human Phosphokinase Array alongside RNA-seq analysis. The phosphorylation assay revealed that luteolin inhibits cell proliferation by decreasing CREB phosphorylation and increasing p53 phosphorylation at ser15 and ser46. Furthermore, RNA-seq analysis showed that p53 was activated following luteolin and siVRK1 treatments.

p53 activation via phosphorylation at ser15 causes cell cycle arrest during mild cellular damage, whereas apoptosis is induced if both ser15 and ser46 are phosphorylated [18]. VRK1 functions as an early stressor during the p53-mediated DNA damage response and VRK1-p53 autoregulatory loop [14]. Moreover, VRK1 can phosphorylate CREB to stimulate cell proliferation [30]. This indicates that luteolin inhibits the CREB phosphorylation, cell cycle, and apoptosis by inhibiting VRK1 expression. Furthermore, luteolin decreases MDM2 expression, thereby reducing p53 ubiquitination and, in turn, stimulating p53 phosphorylation.

Most HGSOC harbor *TP53* mutations, and the mutated *TP53* might decrease the effect of the p53 signaling pathway. However, as shown in Supplementary Fig. 2, luteolin can decrease cell proliferation in all cell lines with or without *TP53* mutation. Moreover, the human phosphokinase array result shows that luteolin can decrease the phosphorylation of CREB, especially in ES2 which has a *TP53* mutation. These results indicate that in *TP53* mutation cell lines, luteolin inhibits the p53 signaling pathway by downregulating VRK1. However, decreasing the phosphorylation of CREB by downregulating VRK1 might be more effective on cell proliferation. This assumption might be addressed in our future studies.

To the best of our knowledge, this study is the first to evaluate the effects of luteolin in a PDX model. Animal experiments demonstrated the synergistic effects of luteolin and cisplatin in vivo. The effect of the intraperitoneal injection of luteolin in combination with cisplatin is better than that of cisplatin alone. The effects of the oral administration of luteolin on HGSOC have also been demonstrated. Furthermore, based on the body weight of mice, immunohistochemistry of phosphorylated p53 (ser15), and western blots of HOSE1C and HOSE2C both with and without luteolin treatment, luteolin was demonstrated as potentially nontoxic to normal tissues. According to the food that mice ate every day, we can calculate how much a normal person needs every day, and the concentration of luteolin is achievable by taking luteolin supplements. The oral administration of luteolin is thus a potential tumor growth suppressor.

Thus, the findings of this study show that luteolin, a natural flavonoid, significantly inhibits the proliferation of HGSOC cells both in vitro and in vivo. Luteolin suppresses HGSOC cell proliferation by decreasing VRK1 expression, thereby rendering the cells susceptible to apoptosis and cell cycle arrest through the upregulation of the p53 signaling pathway. We confirmed the tumor-suppressing effects of luteolin both through intraperitoneal injection and oral administration. Luteolin can also increase the effect of cisplatin on tumor inhibition. Specifically, as the oral administration of luteolin also suppresses HGSOC progress in mice, this may be a more convenient route of administration than intraperitoneal injection in maintenance treatment.

Funding

This work was supported in part by the Japan Society for the Promotion of Science KAKENHI grant number 20K18162 (Grant-in-Aid for Young Scientists), a research grant from the SGH Foundation (2020), and a grant from Uehara Memorial Foundation (2020) awarded to Satoshi Tamauchi.

Ethics approval and consent to participate

This study protocol was approved by the ethics committee of our institute (approval nos. 2015–0237).

CRediT authorship contribution statement

Xuboya Chang: Conceptualization, Methodology, Software, Validation, Data curation, Writing – original draft, Writing – review & editing. **Satoshi Tamauchi:** Conceptualization, Formal analysis, Funding acquisition, Project administration, Visualization, Writing – original draft, Writing – review & editing. **Kosuke Yoshida:** Data curation, Methodology, Visualization, Writing – review & editing. **Masato Yoshihara:** Formal analysis, Supervision, Writing – review & editing. **Akira Yokoi:** Formal analysis, Supervision, Writing – review & editing. **Yusuke Shimizu:** Formal analysis, Supervision, Writing – review & editing. **Yoshiki Ikeda:** Formal analysis, Supervision, Writing – review & editing. **Nobuhisa Yoshikawa:** Formal analysis, Supervision, Writing – review & editing. **Tohru Kiyono:** Formal analysis, Supervision, Writing – review & editing. **Yusuke Yamamoto:** Formal analysis, Supervision, Writing – review & editing. **Hiroaki Kajiyama:** Formal analysis, Supervision, Writing – review & editing.

Declaration of Competing Interest

The authors report no conflict of interest.

Acknowledgments

We thank Enago (https://www.enago.jp/) for English editing of this manuscript.

This work was financially supported by JST SPRING, Grant Number JPMJSP2125. The author (Initial) would like to take this opportunity to thank the “Interdisciplinary Frontier Next-Generation Researcher Program of the Tokai Higher Education and Research System.”

Fig. 4. Oral luteolin suppresses tumor growth in vivo.
A. Images of tumors from a PDX model treated with PBS or luteolin administered orally.
B. Tumor volume in mice fed with normal food or luteolin-containing food (50 ppm) ($n = 6$ /group).
C. Body weight of mice.
D. Expression of phosphorylated histone H3 (ser10) and phosphorylated p53 (ser53) in tumors from a PDX model via immunohistochemistry. Scale bar: 50 um.
E. Graphic illustration of the inhibitory effect of luteolin on cell proliferation mediated by the p53 signaling pathway.

Appendix A. Supplementary data

Supplementary data to this article can be found online at https://doi.org/10.1016/j.ygyno.2023.04.003.

References

[1] R.L. Siegel, K.D. Miller, A. Jemal, Cancer statistics, 2018, CA Cancer J. Clin. 68 (2018) 7–30, https://doi.org/10.3322/caac.21442.

[2] L.A. Torre, B. Trabert, C.E. DeSantis, K.D. Miller, G. Samimi, C.D. Runowicz, M.M. Gaudet, A. Jemal, R.L. Siegel, Ovarian cancer statistics, 2018, CA Cancer J. Clin. 68 (2018) 284–296, https://doi.org/10.3322/caac.21456.

[3] I. Romero, R.C. Bast, Minireview: human ovarian Cancer: biology, current management, and paths to personalizing therapy, Endocrinology. 153 (2012) 1593–1602, https://doi.org/10.1210/en.2011-2123.

[4] O. Oyebode, V. Gordon-Dseagu, A. Walker, J.S. Mindell, Fruit and vegetable consumption and all-cause, cancer and CVD mortality: analysis of health survey for England data, J. Epidemiol. Community Health 68 (2014) (1978) 856–862, https://doi.org/10.1136/jech-2013-203500.

[5] R.K. Ambasta, R. Gupta, D. Kumar, S. Bhattacharya, A. Sarkar, P. Kumar, Can luteolin be a therapeutic molecule for both colon cancer and diabetes? Brief. Funct. Genomics 18 (2019) 230–239, https://doi.org/10.1093/bfgp/ely036.

[6] L.Q. Ren, Q. Li, Y. Zhang, Luteolin suppresses the proliferation of gastric cancer cells and acts in synergy with oxaliplatin, Biomed. Res. Int. 2020 (2020), https://doi.org/10.1155/2020/9396512.

[7] N.A. Soliman, R.N. Abd-Ellatif, A.A. ELSaadany, S.M. Shalaby, A.E. Bedeer, Luteolin and 5-flurouracil act synergistically to induce cellular weapons in experimentally induced solid Ehrlich carcinoma: realistic role of P53; a guardian fights in a cellular battle, Chem. Biol. Interact. 310 (2019), 108740, https://doi.org/10.1016/j.cbi.2019.108740.

[8] M. Zang, L. Hu, Z. Fan, H. Wang, Z. Zhu, S. Cao, X. Wu, J. Li, L. Su, C. Li, Z. Zhu, M. Yan, B. Liu, Luteolin suppresses gastric cancer progression by reversing epithelial-mesenchymal transition via suppression of the notch signaling pathway, J. Transl. Med. 15 (2017) 52, https://doi.org/10.1186/s12967-017-1151-6.

[9] G. Wu, J. Li, J. Yue, S. Zhang, K. Yunusi, Liposome encapsulated luteolin showed enhanced antitumor efficacy to colorectal carcinoma, Mol. Med. Rep. 17 (2018) 2456–2464, https://doi.org/10.3892/mmr.2017.8185.

[10] K. Iida, T. Naiki, A. Naiki-Ito, S. Suzuki, H. Kato, S. Nozaki, T. Nagai, T. Etani, Y. Nagayasu, R. Ando, N. Kawai, T. Yasui, S. Takahashi, Luteolin suppresses bladder cancer growth via regulation of mechanistic target of rapamycin pathway, Cancer Sci. 111 (2020) 1165–1179, https://doi.org/10.1111/cas.14334.

[11] Y.S. Kim, S.H. Kim, J. Shin, A. Harikishore, J.K. Lim, Y. Jung, H.N. Lyu, N.I. Baek, K.Y. Choi, H.S. Yoon, K.T. Kim, Luteolin suppresses cancer cell proliferation by targeting vaccinia-related kinase 1, PLoS One 9 (2014) https://doi.org/10.1371/journal.pone.0109655.

[12] Z.C. Liu, K. Cao, Z.H. Xiao, L. Qiao, X.Q. Wang, B. Shang, Y. Jia, Z. Wang, VRK1 promotes cisplatin resistance by up-regulating c-MYC via c-Jun activation and serves as a therapeutic target in esophageal squamous cell carcinoma, Oncotarget. 8 (2017) 65642–65658, https://doi.org/10.18632/oncotarget.20020.

[13] I. Campillo-Marcos, P.A. Lazo, Implication of the VRK1 chromatin kinase in the signaling responses to DNA damage: a therapeutic target? Cell. Mol. Life Sci. 75 (2018) 2375–2388, https://doi.org/10.1007/s00018-018-2811-2.

[14] I. Campillo-Marcos, R. García-González, E. Navarro-Carrasco, P.A. Lazo, The human VRK1 chromatin kinase in cancer biology, Cancer Lett. 503 (2021) 117–128, https://doi.org/10.1016/j.canlet.2020.12.032.

[15] F.M. Behan, F. Iorio, G. Picco, E. Gonçalves, C.M. Beaver, G. Migliardi, R. Santos, Y. Rao, F. Sassi, M. Pinnelli, R. Ansari, S. Harper, D.A. Jackson, R. McRae, R. Pooley, P. Wilkinson, D. van der Meer, D. Dow, C. Buser-Doepner, A. Bertotti, L. Trusolino, E.A. Stronach, J. Saez-Rodriguez, K. Yusa, M.J. Garnett, Prioritization of cancer therapeutic targets using CRISPR–Cas9 screens, Nature. 568 (2019) 511–516, https://doi.org/10.1038/s41586-019-1103-9.

[16] K. Yoshida, N. Yoshikawa, K. Kitami, S. Tamauchi, Y. Ikeda, A. Yokoi, K. Nishino, K. Niimi, H. Kajiyama, Metabolome analysis reveals a diversity of cancer tissues in advanced epithelial ovarian cancer, Cancer Cell Int. 21 (2021) 1–8, https://doi.org/10.1186/s12935-021-02014-7.

[17] Q. Luo, J.M. Beaver, Y. Liu, Z. Zhang, Dynamics of p53: a master decider of cell fate, Genes (Basel) 8 (2017), https://doi.org/10.3390/genes8020066.

[18] S.J. Arief Ichwan, M. Taher, K. Ohtani, M.-A. Ike, Therapeutic targeting of p53-mediated apoptosis pathway in head and neck squamous cell carcinomas: Current progress and challenges, Tumor Suppressor Genes, InTech, 2012, https://doi.org/10.5772/27968.

[19] J. Erriquez, M. Olivero, G. Mittica, M.S. Scalzo, M. Vaira, M. de Simone, R. Ponzone, D. Katsaros, M. Aglietta, R. Calogero, M.F. di Renzo, G. Valabrega, Xenopatients show the need for precision medicine approach to chemotherapy in ovarian cancer, Oncotarget. 7 (2016) 26181–26191, https://doi.org/10.18632/oncotarget.8325.

[20] J.M. Santiago-O'Farrill, S.J. Weroha, X. Hou, A.L. Oberg, E.P. Heinzen, M.J. Maurer, L. Pang, P. Rask, R.K. Amaravadi, S.E. Becker, I. Romero, M.J. Rubio, X. Matias-Guiu, M. Santacana, A. Llombart-Cussac, A. Poveda, Z. Lu, R.C. Bast, Poly(adenosine diphosphate ribose) polymerase inhibitors induce autophagy-mediated drug resistance in ovarian cancer cells, xenografts, and patient-derived xenograft models, Cancer. 126 (2020) 894–907, https://doi.org/10.1002/cncr.32600.

[21] S.J. Weroha, M.A. Becker, S. Enderica-Gonzalez, S.C. Harrington, A.L. Oberg, M.J. Maurer, S.E. Perkins, M. AlHilli, K.A. Butler, S. McKinstry, S. Fink, R.B. Jenkins, X. Hou, K.R. Kalli, K.M. Goodman, J.N. Sarkaria, B.Y. Karlan, A. Kumar, S.H. Kaufmann, L.C. Hartmann, P. Haluska, Tumorgrafts as in vivo surrogates for women with ovarian cancer, Clin. Cancer Res. 20 (2014) 1288–1297, https://doi.org/10.1158/1078-0432.CCR-13-2611.

[22] R. Sasaki, M. Narisawa-Saito, T. Yugawa, M. Fujita, H. Tashiro, H. Katabuchi, T. Kiyono, Oncogenic transformation of human ovarian surface epithelial cells with defined cellular oncogenes, Carcinogenesis. 30 (2009) 423–431, https://doi.org/10.1093/carcin/bgp007.

[23] C. Ricciardelli, N.A. Lokman, I. Sabit, K. Gunasegaran, W.M. Bonner, C.E. Pyragius, A.M. Macpherson, M.K. Oehler, Novel ex vivo ovarian cancer tissue explant assay for prediction of chemosensitivity and response to novel therapeutics, Cancer Lett. 421 (2018) 51–58, https://doi.org/10.1016/j.canlet.2018.02.006.

[24] T. Maeda, H. Tashiro, H. Katabuchi, M. Begum, H. Ohtake, T. Kiyono, H. Okamura, Establishment of an immortalised human ovarian surface epithelial cell line without chromosomal instability, Br. J. Cancer 93 (2005) 116–123, https://doi.org/10.1038/sj.bjc.6602662.

[25] J. Liu, Y. Wang, S. He, X. Xu, Y. Huang, J. Tang, Y. Wu, X. Miao, Y. He, Q. Wang, L. Liang, C. Cheng, Expression of vaccinia-related kinase 1 (VRK1) accelerates cell proliferation but overcomes cell adhesion mediated drug resistance (CAM-DR) in multiple myeloma, Hematology. 21 (2016) 603–612, https://doi.org/10.1080/10245332.2016.1147678.

[26] M. López-Lázaro, Distribution and Biological Activities of the Flavonoid Luteolin, 2009.

[27] D. Hanahan, R.A. Weinberg, Hallmarks of cancer: the next generation, Cell. 144 (2011) 646–674, https://doi.org/10.1016/j.cell.2011.02.013.

[28] B. van Zyl, D. Tang, N.A. Bowden, N. Bowden, Biomarkers of Platinum Resistance in Ovarian cancer: What Can we Use to Improve 1 Treatment, 2018.

[29] A.M. Mon, A. Craig MacKinnon, P. Traktman, Overexpression of the VRK1 kinase, which is associated with breast cancer, induces a mesenchymal to epithelial transition in mammary epithelial cells, PLoS One 13 (2018), https://doi.org/10.1371/journal.pone.0203397.

[30] T.H. Kang, D.Y. Park, W. Kim, K.T. Kim, VRK1 phosphorylates CREB and mediates CCND1 expression, J. Cell Sci. 121 (2008) 3035–3041, https://doi.org/10.1242/jcs.026757.